Since January 2020 Elsevier has created a COVID-19 resource centre with free information in English and Mandarin on the novel coronavirus COVID-19. The COVID-19 resource centre is hosted on Elsevier Connect, the company's public news and information website.

Bioorganic & Medicinal Chemistry Letters 29 (2019) 126727

Contents lists available at ScienceDirect

Bioorganic & Medicinal Chemistry Letters

journal homepage: www.elsevier.com/locate/bmcl

Synthesis and biological evaluation of 3-acyl-2-phenylamino-1,4-dihydroquinolin-4(1*H*)-one derivatives as potential MERS-CoV inhibitors

Ji Hye Yoon[a], Jun Young Lee[a], Jihye Lee[b], Young Sup Shin[a], Sangeun Jeon[b], Dong Eon Kim[c], Jung Sun Min[c], Jong Hwan Song[a], Seungtaek Kim[d], Sunoh Kwon[c], Young-hee Jin[c], Min Seong Jang[e], Hyoung Rae Kim[a], Chul Min Park[a,*]

[a] *Center for Convergent Research of Emerging Virus Infection (CEVI), Korea Research Institute of Chemical Technology, 141 Gajeong-ro, Yuseong-gu, Daejeon 34114, South Korea*
[b] *Respiratory Virus Laboratory, Institut Pasteur Korea, Seongnam-si, Gyeonggi-do 13488, South Korea*
[c] *Herbal Medicine Research Division, Korea Institute of Oriental Medicine, Daejeon 34054, South Korea*
[d] *Zoonotic Virus Laboratory, Institut Pasteur Korea, Seongnam-si, Gyeonggi-do 13488, South Korea*
[e] *Department of Non-Clinical Studies, Korea Institute of Toxicology, Yuseong-gu, Daejeon 34114, South Korea*

ARTICLE INFO

Keywords:
MERS-CoV
RNA virus
3-Acyl-2-amino-1,4-dihydroquinolin-4(1*H*)-ones
Inhibitor
SAR optimization

ABSTRACT

3-Acyl-2-phenylamino-1,4-dihydroquinolin-4(1*H*)-one derivatives were synthesized and evaluated to show high anti-MERS-CoV inhibitory activities. Among them, 6,8-difluoro-3-isobutyryl-2-((2,3,4-trifluorophenyl)amino) quinolin-4(1*H*)-one (**6u**) exhibits high inhibitory effect (IC_{50} = 86 nM) and low toxicity (CC_{50} > 25 μM). Moreover, it shows good metabolic stability, low hERG binding affinity, no cytotoxicity, and good *in vivo* PK properties.

Middle East respiratory syndrome coronavirus (MERS-CoV) is an emerging, fatal virus that causes severe respiratory symptoms in humans with high mortality (about 38%), such as high fever, cough, shortness of breath, and acute pneumoniae.[1,2] MERS-CoV is a zoonotic coronavirus that can spread non-sustained person-to-person transmission.[3] Travel-related MERS-CoV infections continued to spread from the Arabian Peninsula to several other countries and caused epidemics with high fatal rates.[4]

MERS-CoV is a single-stranded, positive-sense RNA virus and uses host cellular components to accomplish various physiological processes, including internalization of the virion, genome replication, packaging and budding of the virions. Therefore, each stage of these steps of the virus life cycle can be targets for therapeutic inhibition. Screening of FDA-approved drugs for MERS-CoV identified many drugs with antiviral effects.[5,6] These drugs can be categorized into inhibitors disrupting endocytosis, interrupting MERS-CoV RNA replication and translation, and inhibitors with undefined mechanisms. To date, there are still no approved antiviral drugs.[2] Therefore, the development of therapeutics against MERS has received more and more attention.

We began our investigation by screening 200,000 compounds of Korean Chemical Bank (KCB) against MERS-CoV using high content screening (HCS) platform of Institut Pasteur Korea (IPK).[7] Through this effort, 3-acetyl-6-chloro-2-(isopropylamino)-8-(trifluoromethyl)quinolin-4(1*H*)-one **1** was identified as a primary hit (Fig. 1). 1,4-Dihydroquinolin-4-one derivatives showed a broad range of pharmacological activities, such as antibacterial,[8] anti-neurodegenerative,[9] and anti-infammatory.[10] Here we report on the synthesis and biological effects of 3-acyl-2-amino-1,4-dihydroquinolin-4(1*H*)-one derivatives.

All series of 3-acyl-2-amino-1,4-dihydroquinolin-4-one analogues were synthesized using Scheme 1. β-Keto amides **2** were prepared either by reaction of diketene and anilines in the presence of basic catalyst or condensation reaction of substituted-acetyl acetate and anilines. Bis(methylthio) compounds **3** were synthesized by reacting β-keto amides **2** with carbon disulfide and dimethylsulfate in the presence of potassium carbonate. Refluxing bis(methylthio) compounds **3** in an inert solvent like 1,2-dichlorobenzene was transformed into 3-acyl-2-methylsulfanyl-quinoline-4(1*H*)-ones **4**.[11] Treatment of 3-acyl-2-methylsulfanyl-quinolin-4(1*H*)-ones **4** with hydrogen peroxide in acetic acid leaded to the corresponding sulfoxides **5**, which are more reactive to substitution reaction. Nucleophilic substitution reactions with various amines with sulfoxides **5** afforded 2-amino-1,4-dihydroquinolin-4(1*H*)-ones **6**.[12]

The anti-MERS-CoV activities of the synthesized compounds for Vero cells infected with a Korean clinical MERS-CoV isolate were

* Corresponding author.

https://doi.org/10.1016/j.bmcl.2019.126727
Received 24 June 2019; Received in revised form 6 September 2019; Accepted 30 September 2019
Available online 09 October 2019
0960-894X/

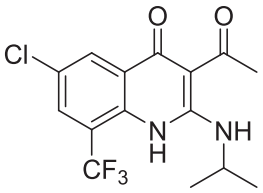

1

IC_{50} : 0.77 μM

CC_{50} : > 25 μM

Fig. 1. Hit compound obtained from HTS.

determined by monitoring the cells expressing viral spike (S) protein using immunofluorescence assay (IFA).[7] Extensive SAR investigations to assess the effects of 3-acyl moieties, substituents on aryl, and various amines are shown in Table 1.

We started SAR studies by varying the substituents of 5 to 8 positions of quinolone ring of compound **1**, having fixed with acetyl group at 3 position and isopropyl amine at 2 position. Compounds with electron donating groups, such as 8-isopropyl (**6a**) and 6,8-dimethyl (**6b**), showed no inhibitory effects. Application of phenyl substituent at 3 position (**6c**) was detrimental for inhibitory effect. 2,4-Difluoroaniline substituent at 2 position (**6d**) resulted in significant higher activity (IC_{50} = 0.15 μM). Given the beneficial effect of 2,4-difluoroaniline at 2 position, we explored the effects of electron-withdrawing groups of left-hand ring of quinolone part of **6d** by preparing analogues **6e–6h**. Replacement of the C(8)-trifluoromethyl with fluorine (**6e**) and nitro functionality at 2 position (**6f**) were moderately tolerated (IC_{50} = 0.98 and 1.16 μM, respectively). 6,8-Difluoro (**6g**) and 5,6,8-trichloro (**6h**) derivatives also retained the inhibitory effects (IC_{50} = 1.06 and 0.29 μM, respectively). This observation showed that electron-withdrawing substituents of left-ring of quinolone scaffold were fruitful to inhibitory activity, while electron-donating substituents were detrimental.

Next, substituent effects at 2 position of 1,4-dihydroquinolin-4(1*H*)-one scaffold were evaluated. Although less active than quinolone derivative **6d** (IC_{50} = 0.15 μM) with 6-chloro-8-trifluoromethyl group, 6,8-difluoro substituent analogue **6g** opens the possibility to extensively explore SAR studies via modifications of 2 position. Therefore, we have focused on the optimization of **6g**. 3-Acetyl-6,8-difluoro-1,4-dihydroquinolin-4(1*H*)-ones with piperidine (**6i**) and morpholine (**6j**), *n*-butyl amine (**6k**) at 2 position showed no inhibitory effect. 3,4-Dichlorobenzyl alcohol (**6l**) and 2,4-difluorobenzyl amine (**6m**) were only moderated tolerated (IC_{50} = 7.8 and 5.9 μM, respectively), whereas 4-fluorobenzyl amine (**6n**) and 4-methoxybenzyl amine (**6o**) functionalities are detrimental for the binding affinities. Compounds with 3-methoxyaniline (**6p**) and 4-methoxyaniline (**6q**) showed no inhibitory effects, indicating that aniline substituents with electron-donating groups were detrimental. 4-Bromoaniline (**6r**) and 4-chloroaniline group (**6s**) showed similar inhibitory effects (IC_{50} = 1.13 and 1.44 μM, respectively) to **6g**. 2,3,4-Trifluoroaniline analogue **6t** displayed increased inhibitory effect (IC_{50} = 0.53 μM). Through the investigation into wide range of substituent effects at 2 position, aniline groups with electron-withdrawing substituents showed high binding affinities (0.53–1.44 μM).

In the next phase of optimization, substituent effects at 3 position were investigated. As the benzoyl substituent (**6c**) at 3 position completely abolished activity and pivaloyl group at 3 position blocked the nucleophilic substitution of anilines at 2 position, compounds with isobutyryl substituent at 3 position were deeply examined (**6u–z**). 6,8-Difluoro Compound **6u** and **6v**, including 2,3,4-trifluoroaniline and 2,4-difluoro aniline group at 2 position, showed higher inhibitory effects than its corresponding compounds with acetyl group at 3 position (IC_{50} = 0.086 and 0.79 μM, respectively). 5,6,8-Trichloro (**6w**) and 5,8-dichloro compound (**6x**) with 2,3,4-trifluoaniline substituent at 2 position also displayed higher inhibitory effects (IC_{50} = 0.100 and 0.166 μM, respectively) than their corresponding ones. 5,6,8-Trichloro (**6y**) and 6-chloro,8-trifluoro compound (**6z**) with 2,4-difluoroaniline substituent at 2 position also showed potent biological activities (IC_{50} = 0.129 and 0.13 μM, respectively). Of note, all the above compounds except **6d**, **6w**, and **6z** displayed no obvious cytotoxicity (CC_{50} > 10 μM).

Compound **6u** was found to be a very potent MERS-CoV inhibitor and evaluated further for its metabolic stability, hERG, cytotoxicity, and *in vivo* pharmacokinetic profile (Table 2). **6u** displays good metabolic stability in human, rat, and mouse liver microsomes. **6u** shows a low hERG binding affinity and no cytotoxicity toward VERO, HFL-1, L929, NIH 3T3, and CHO-K1 cell lines and it exhibits good oral bioavailability of 56% with promising C_{max}, $T_{1/2}$, AUC values and clearance.

In Summary, we have developed a novel class of 3-acyl-2-amino-1,4-dihydroquinolin-4(1*H*)-one based MERS-CoV inhibitors through systemic SAR optimization from lead compound **1**. Compound **6u**, including isobutyryl substituent at 3 position and 6,8-difluorophenyl group, is a good MERS-CoV inhibitor with IC_{50} of 86 nM. In addition, this substance shows good metabolic stability, low hERG binding affinity, no cytotoxicity, and good *in vivo* PK properties with an oral bioavailability of 56% in rat. Future optimization of these 3-acyl-2-amino-1,4-dihydroquinolin-4(1*H*)-one based MERS-CoV inhibitors on

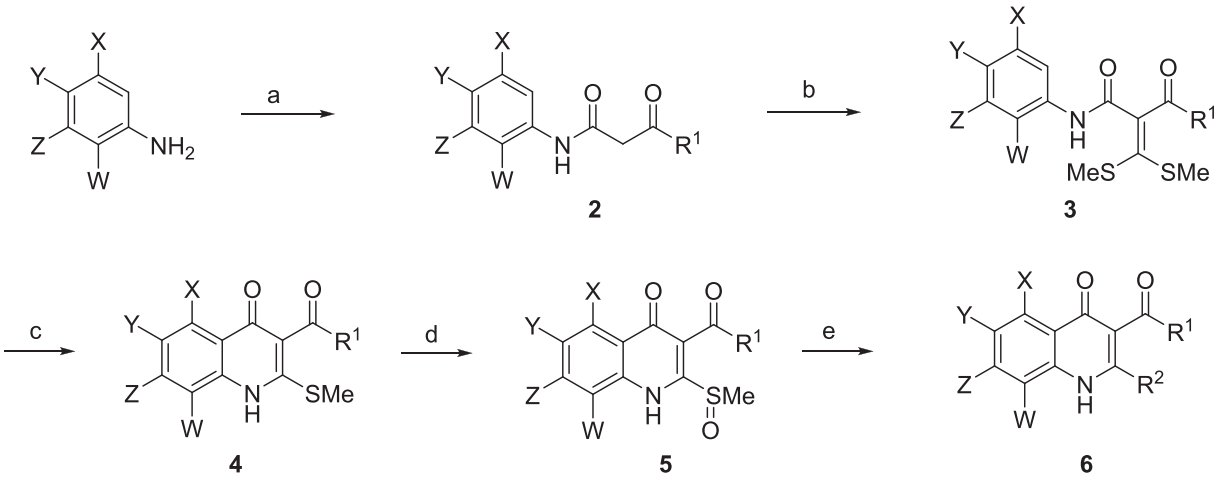

Scheme 1. Synthesis pathway towards derivatives **6**. Reagents and conditions: (a) Diketene, Et_3N, benzene, 110 °C; or Substituted-acetyl acetate, Et_3N, toluene, 125 °C; (b) CS_2, Dimethyl sulfate, n-Bu_4NBr, K_2CO_3, DMF, rt; (c) o-Dichlorobenzene, 180 °C; (d) H_2O_2, AcOH, 50 °C; (e) Amines or alcohol, Ph_2O, 180 °C.

Table 1
MERS-CoV inhibitory activity of 3-acyl-2-amino-1,4-dihydroquinolin-4(1*H*)-one derivatives.

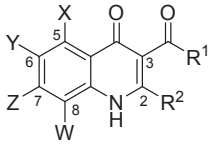

6

Cpd	X	Y	Z	W	R^1	R^2	IC_{50} (μM)[a]	CC_{50} (μM)[b]	SI[c]
1	H	Cl	H	CF_3	Me	i-PrNH-	0.77	> 25	33
6a	H	H	H	i-Pr	Me	i-PrNH-	> 25	–	–
6b	H	Me	H	Me	Me	i-PrNH-	> 25	–	–
6c	H	Cl	H	CF_3	Ph	i-PrNH-	> 25	–	–
6d	H	Cl	H	CF_3	Me	2,4-F_2-PhNH-	0.15	7.3	78
6e	H	Cl	H	F	Me	2,4-F_2-PhNH-	0.98	> 25	26
6f	H	Cl	H	NO_2	Me	2,4-F_2-PhNH-	1.16	> 25	21
6g	H	F	H	F	Me	2,4-F_2-PhNH-	1.06	> 25	25
6h	Cl	Cl	H	Cl	Me	2,4-F_2-PhNH-	0.29	> 25	91
6i	H	F	H	F	Me	1-Piperidinyl	> 25	> 25	1
6j	H	F	H	F	Me	4-Morpholinyl	> 25	> 25	1
6k	H	F	H	F	Me	*n*-ButylNH-	> 25	> 25	1
6l	H	F	H	F	Me	3,4-Cl_2-$PhCH_2O$-	7.8	> 25	3
6m	H	F	H	F	Me	2,4-F_2-$PhCH_2NH$-	5.9	> 25	3
6n	H	F	H	F	Me	4-F-$PhCH_2NH$-	17.6	> 25	1
6o	H	F	H	F	Me	4-MeO-$PhCH_2NH$-	> 25	> 25	1
6p	H	F	H	F	Me	3-MeO-PhNH-	> 25	> 25	1
6q	H	F	H	F	Me	4-MeO-PhNH-	> 25	> 25	1
6r	H	F	H	F	Me	4-Br-PhNH-	1.13	> 25	28
6s	H	F	H	F	Me	4-Cl-PhNH-	1.44	> 25	22
6t	H	F	H	F	Me	2,3,4-F_3-PhNH-	0.53	> 25	48
6u	H	F	H	F	i-Pr	2,3,4-F_3-PhNH-	0.086 ± 0.041[d]	> 25	500
6v	H	F	H	F	i-Pr	2,4-F_2-PhNH-	0.79	> 25	45
6w	Cl	Cl	H	Cl	i-Pr	2,3,4-F_3-PhNH-	0.100 ± 0.023[d]	6.4	77
6x	Cl	H	H	Cl	i-Pr	2,3,4-F_3-PhNH-	0.166 ± 0.067[d]	10.89 ± 4.29[d]	9
6y	Cl	Cl	F	Cl	i-Pr	2,4-F_2-PhNH-	0.129 ± 0.026[d]	> 25	231
6z	H	Cl	H	CF_3	i-Pr	2,4-F_2-PhNH	0.13	7.3	144

[a,b] IC_{50} and CC_{50} were derived from the results of at least two independent experiment in VERO.
[c] SI (selectivity index) = CC_{50}/IC_{50} for inhibiting MERS-CoV infection.
[d] Mean ± SD of four independent tests.

Table 2
Data for microsomal stability, hERG, cytotoxicity, and *in vivo* pharmacokinetic profile of **6u**.

Assay	Results of **6u**
Human microsomal stability[a]	52
Rat microsomal stability[a]	44
Mouse microsomal stability[a]	35
hERG[b]	6.9
Cytotoxicity[c]	VERO: 86.1
	HFL-1: 15.6
	L929: 15.8
	NIH 3 T3: 65.6
	CHO-K1: 6.9
In vivo PK[d]	
C_{max} (μg/mL)	2.32 ± 0.20
$T_{1/2}$ (h), i.v.	4.6 ± 0.66
AUC_{0-24h} (μg·h/mL), i.v.	28.3 ± 4.18
$AUC_{0-\infty}$ (μg·h/mL), i.v.	28.9 ± 4.21
CL (L/h/kg), i.v.	0.07 ± 0.01
%F	56

[a] % original compound remained after 30 min incubation.
[b] IC_{50} (μM) values (binding assay).
[c] IC_{50} (μM) values in various mammalian cell lines. Cell information. VERO: African green monkey kidney cell line, HFL-1: human embryonic lung cell line, L929: mouse fibroblast cell line, NIH 3T3: mouse embryonic fibroblast cell line, CHO-K1: Chinese hamster ovary cell line.
[d] Data were generated in rats from three determinations, and dosed at 2 mg/kg for i.v. and at 5 mg/kg for p.o. (n = 3).

the *in vivo* efficacy of **6u** in animal models will mainly be performed in due course.

Declaration of Competing Interest

The authors declare that they have no known competing financial interests or personal relationships that could have appeared to influence the work reported in this paper.

Acknowledgements

The chemical library used in this study was kindly provided by Korea Chemical Bank (http://www.chemicalbank.org/) of Korea Research Institute of Chemical Technology. This work was supported by a grant of National Research Council of Science & Technology (NST) by the Korean government (MSIP) (No. CRC-16-01-KRICT).

Appendix A. Supplementary data

Supplementary data to this article can be found online at https://doi.org/10.1016/j.bmcl.2019.126727.

References

1. Cotten M, Watson SJ, Zumla AI, et al. *mBio.* 2014;5:e01062–e01063.
2. Liang R, Wang L, Zhang N, et al. *Viruses.* 2018;10:721.

3. Chan JFW, Lau SKP, To KKW, Cheng VCC, Woo PCY, Yuen K-Y. *Clin Microbiol Rev.* 2015;28:465.
4. De Wit E, van Doremalen N, Falzarano D, Munster VJ. *Nat Rev Microbiol.* 2016;14:523.
5. Dyall J, Coleman CM, Hart BJ, et al. *Antimicrob Agents Chemother.* 2014;58(8):4885.
6. de Wilde AH, Jochmans D, Posthuma CC, et al. *Antimicrob Agents Chemother.* 2014;58(8):4875.
7. (a) Cruz DJ, Bonotto RM, Gomes RG, et al. *PLoS Negl Trop Dis.* 2013;7(10):2471
(b) Anti-MERS-CoV activity assay. Vero cells were seeded in 384-well μ-clear plates (Greiner Bio-One, Austria) at a density of 1.2×10^4 cell per well in 30 μl SFM and incubated for 24 h prior to infection. Compounds were transferred from the library into intermediate 384-well polypropylene plates containing SFM and were mixed using an automated liquid handling system (Apricot Personal Pipettor, Apricot Design, USA). Subsequently, the diluted compounds were added to the cell plates in 10 μl volumes (final DMSO concentration of 0.5% (v/v)). For infection, the plates were transferred into the BSL-3 containment facility prior to adding 10 μl MERS-CoV at a multiplicity of infection (MOI) of 0.0625. The cells were fixed at 24 hpi with 4% PFA and the infected cells were identified by IFA. The fixed cells were permeabilized with 0.25% Triton X-100 (Sigma-Aldrich, USA) for 20 min. Then the cells were incubated with rabbit anti-MERS-CoV Spike antibody for 1 h at 37°C. After three washes with PBS, the cells were incubated with Alexa 488-conjugated goat anti-rabbit IgG (H + L) secondary antibody and Hoechst 33342 (Life Technologies, USA) for 1 h at 37°C. Images were acquired by Perkin Elmer Operetta (20×; Waltham, USA). The acquired images were analyzed with in-house-developed Image-Mining 3.0 (IM 3.0) plug-in software. In the analyzed image, the total number of cells and the number of infected cells were determined by counting Hoechst-stained nuclei and spike protein-expressing cells, respectively.
8. Kim HJ, Kim N, Shum D, Huddar S, Park CM, Jang S. *Assay Drug Dev Techn.* 2017;15(5):198.
9. Kang D-H, Jun K-Y, Lee JP, Pak CS, Na Y, Kwon Y. *J Med Chem.* 2009;52(9):3093.
10. Sharma MC, Sharma S. *Med Chem Res.* 2016;25:2119.
11. (a) Park CS, Choi EB. *Synthesis.* 1992;12:1291;

(b) Choi EB, Yeon GH, Lee HK, Yang HC, Yoo CY, Park CS. *Synthesis.* 2003;18:2771
(c) **6u**: ^{1}H NMR (300 MHz, $CDCl_3$) δ 13.45 (s, 1H), 7.80 (dt, J = 8.8, 2.2 Hz, 1H), 7.62 (s, 1H), 7.24–7.15 (m, 2H), 7.10 (ddd, J = 10.3, 7.8, 2.8 Hz, 1H), 4.48–4.28 (m, 1H), 1.21 (d, J = 6.7 Hz, 6H); ^{13}C NMR (500 MHz, $CDCl_3$) δ 209.41, 174.51, 159.10, 157.13, 154.38, 151.00, 149.81, 149.02, 127.14, 121.55, 119.85, 113.32, 108.23, 107.16, 106.93, 100.62, 38.98, 19.17; HRMS *m/e* calcd for $C_{19}H_{13}F_5N_2O_2$ $[M]^+$ 396.0897; found 396.0910.
12. Hwang BH, Park SH, Choi EB, Park CS, Lee HK. *Tetrahedron.* 2008;64:6698.